Compressibility of Gas Mixtures

Carbon Dioxide–Ethylene System

A. SASS[1], B. F. DODGE, and R. H. BRETTON
Yale University, New Haven, Conn.

PVT data were obtained for the carbon dioxide–ethylene system at 40°, 50°, 75°, 100°, and 125° C., at pressures from 5 to 500 atm. Mixtures of approximately 20, 40, 60, and 80 mole % ethylene and the two pure components were investigated by use of the Burnett method. Compressibility factors obtained from experimental data are tabulated and smoothed results are reported as polynomials in density. The experimental data were used to obtain the second virial coefficients for the pure gases and the mixtures, and the constants for the Benedict-Webb-Rubin equation of state were evaluated for the pure components and the four mixtures in the temperature range of 50° to 125° C. The rules for combining constants to predict mixture behavior proposed by Benedict, Webb, and Rubin were inadequate for this system.

EXPERIMENTAL STUDIES on the pressure-volume-temperature (*PVT*) properties of gases have been carried out for well over 100 years. However, this area of investigation is still important for the chemical engineer, since it is still not possible to predict accurately, by theoretical or empirical means, the *PVT* properties of all gas systems. This shortcoming is particularly acute for systems containing more than one component. Since the impossibility of studying experimentally all the possible multicomponent gas systems is evident, correlations must be developed which will allow prediction of the *PVT* properties of gas mixtures based on a knowledge of the properties of the pure components. At present, accurate mixing rules are available for only a few special systems. Before more general and more accurate correlations can be developed, experimental data on many different multicomponent systems must be available. The purpose of this research was to provide accurate *PVT* data on a gas mixture which had not been thoroughly investigated previously and to point out some of the shortcomings of the mixing rules which are now available.

The carbon dioxide–ethylene system was chosen because few other binary mixtures have been studied in which both molecules have a complex molecular configuration. Data were taken at pressures up to 500 atm. and temperatures from 40° to 125° C. The technique used to obtain the data is known as the Burnett method (*4*). It is ingenious, since one can obtain the *PVT* properties of a gas without directly measuring the mass or volume of the gas. Only temperature and pressure measurements are required.

PREVIOUS WORK

Compressibility Measurements. The most comprehensive study of the compressibility of ethylene is that of Michels, DeGruyter, and Niesen (*18*) and Michels and Geldermanns (*19*), who investigated the compressibility from 20 to 3000 atm. at temperatures from 0° to 150° C. The other available data are limited in their usefulness because of the small ranges investigated or the lack of accuracy of the work. These data were reviewed by Dick and Hedley (*5*).

Michels and Michels (*20*) studied the compressibility of carbon dioxide from 16 to 3000 atm. at temperatures from 0° to 150° C. Another comprehensive study of carbon dioxide is that of Reamer, Sage, and Lacey (*26*), who studied the compressibility to 10,000 p.s.i. from 100° to 460° F. at 60° intervals. MacCormack and Schneider (*17*) covered the temperature range 0° to 600° C. and pressure range 1 to 50 atm. in their investigation of carbon dioxide. A review of the available literature is given by Newitt and Pai (*22*).

The only data available on carbon dioxide–ethylene mixtures in the temperature range of this investigation are those of Ku (*12*), who studied three mixtures, 12, 25, and 70 mole % carbon dioxide, at 100° C. and pressures up to 260 atm.

DISCUSSION OF BURNETT METHOD

Basic Equations. Since the derivation of the basic Burnett equations has been presented many times in the literature, only the final equations used to calculate the compressibility factor are listed here.

$$Z_n = \frac{N^n P_n}{A} \qquad (1)$$

$$A = \lim_{P \to 0} N^n P_n \frac{P_0}{Z_0} \qquad (2)$$

For many gas systems, including the one studied in this investigation, the plot of $N^n P_n$ *vs.* P_n is nonlinear in the low-pressure range. To obtain an accurate extrapolation to the limit at $P = 0$ we used an analytical method which used the data in the region below 50 to 60 atm.

When limited to this pressure range, it is possible to represent the compressibility behavior of most systems by a number of very simple equations of state. The one which we found most useful had been used by Harper and Miller (*8*) and has the form:

$$\ln Z = B'P + C'P^2 + D'P^3 \ldots \qquad (3)$$

The coefficients of this series can be directly related to the coefficients in the more familiar virial equation

$$Z = 1 + BP + CP^2 + DP^3 \ldots \qquad (4)$$

as follows:

$$B' = B \qquad (5)$$

---

[1] Present address: Applied Research Laboratory, United States Steel Corp., Monroeville, Pa.

$$C' = C - B^2/2 \tag{6}$$

$$D' = D - BC + B^3/3 \tag{7}$$

If Equation 3 is combined with Equation 1, one obtains

$$\ln P_n = \ln A - n \ln N + B'P + C'P^2 + \ldots \tag{8}$$

This equation is linear in the unknowns ln A, B', C', ... Therefore, it is readily susceptible to a least squares analysis.

In practice the compressibility data of carbon dioxide and ethylene up to a pressure of 50 to 60 atm. could be represented by only two terms of the series in Equation 3. The low pressure expansion data were then fitted to the truncated form of Equation 8 by a least squares technique to obtain the value of A.

Modification of Burnett Method. One of the major disadvantages of the Burnett method as usually applied is the poor distribution of the data points. To reduce the severity of the problem, an assembly of three interconnected pressure vessels designated V_1, V_2, and V_3 was used. This modification had been used by Heichelheim and McKetta (*9*). At the higher pressures, the gases were expanded from V_1 into V_2. The volumetric constant for this case was 1.135. At the lower pressures, the gases were expanded from V_1 into V_3, with the resulting value of N equal to 1.377. This arrangement gives a better distribution of data than is possible with the usual Burnett apparatus. However, it is necessary to modify slightly some of the Burnett equations which were presented previously.

Preparation of Gas Mixtures. With the Burnett method, it was possible to prepare the gas mixtures in the pressure vessel and to determine the composition of the mixture from experimental compressibility data. The details of this technique have been presented by Ku (*12*).

Pressure Distortion of Vessels. In the derivation of the Burnett equations, it is assumed that the volumes of the pressure vessels do not change when they are pressurized. Since the volumes of the vessels do increase because of pressure, a correction should be applied. Since this correction is negligible up to pressures of approximately 250 atm., it was applied only for the high pressure expansions from vessel V_1 into vessel V_2. The corrections at the maximum pressures changed the computed compressibility factors by about 0.1%.

EXPERIMENTAL EQUIPMENT

Outline of Operating Procedure. Figure 1 is a schematic diagram of the apparatus. Vessel V_1 is filled with gas from one of the gas cylinders, J. To generate a greater pressure in V_1, the liquid-piston pump, C, D, is used. After allowing time for the gas to attain temperature equilibrium, the pressure of the gas in V_1 is measured by using one of the dead-weight piston gages, E, F, and the diaphragm pressure indicator, N. If a mixture is being prepared, the second component is charged into V_1 by use of the liquid-piston pump. After allowing sufficient time for mixing, the final pressure of the mixture is measured.

The gas in V_1 is then expanded into vessel V_2, which has been previously evacuated. After closing valve 1, the pressure in V_1 is again measured. The contents of V_2 are exhausted to the atmosphere, and the vessel is evacuated. The gas in V_1 is again expanded into V_2 and the new pressure is measured. This procedure of expansion followed by pressure measurement is continued until the pressure in V_1 is approximately 5 or 6 atm.

Pressure-Generating System. The pressure-generating system consists of a liquid-piston pump, C, D, and a 10,000-p.s.i. hydropump, A. It is used to increase the pressure in vessel V_1 above that of the commercial gas cylinder pressure.

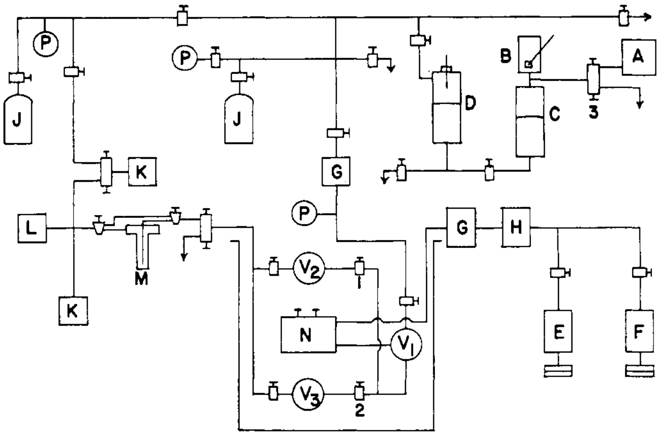

Figure 1. Schematic Diagram of the Apparatus

A. 10,000 p.s.i. air hydropump
B. 10,000 p.s.i. Blackhawk hand pump
C. Oil leg of liquid-piston pump
D. Gas leg of liquid-piston pump
E. High-range dead weight piston gage
F. Low-range dead weight piston gage
G. Mercury traps
H. Open-tube manometer
J. Commercial gas cylinders
K. Vacuum pumps
L. Vacuum gage
M. Cold trap
N. Diaphragm pressure indicator
P. Pressure gages
V. Pressure vessels

The function of the liquid-piston pump is to transmit oil pressure to the gas without contaminating the gas with the oil. This is done by separating the oil and gas by mercury. The pump consists of two identical stainless steel vessels in series. An electrode is located at the top of the gas leg of the pump to indicate when the mercury has reached the top of the vessel. The hydropump, A, is used to generate the necessary pressure in the oil leg of the pump.

More detailed information about this system, as well as the other equipment described, is given by Ku (*12*).

Pressure Vessels. Vessels V_1 and V_3, which were designed and built by Ku, are made from 2-inch stainless steel rod and have an inside diameter of 1 inch. Their volumes are approximately 61 and 26 cc., respectively. Vessel V_2, which was constructed for this investigation, was also made of 2-inch stainless steel rod but has an inside diameter of ½ inch. Its volume is approximately 6 cc.

Pressure-Measuring System. DEAD-WEIGHT PISTON GAGES. To cover the pressure range of this study, it was necessary to use two dead-weight piston gages. The low-range gage was used in the pressure range of 5 to 170 atm., with a 17/64-inch piston which was calibrated by Ku against the vapor pressure of carbon dioxide at 0° C. The high-range gage, which is provided with a 3/16-inch piston, was calibrated against the low-range gage.

DIAPHRAGM PRESSURE INDICATOR. Until recently, the most common method of measuring gas pressure with a dead-weight piston gage involved the use of a mercury U-tube as the connection between the gas in the system and the oil in the gage. This technique has a number of disadvantages, and a diaphragm pressure indicator was substituted for the U-tube in this investigation. This instrument, built by the Ruska Corp., consists basically of two stainless steel compartments separated by a thin stainless steel diaphragm. One side of the diaphragm is exposed to gas pressure, and the other to the oil pressure. The mechanical movement of the diaphragm, due to an overpressure on either side, is electronically detected. The maximum sensitivity of the instrument is approximately 0.01 p.s.i. at atmospheric pressure. Therefore, the uncertainty due to the indicator sensitivity is less than 0.01% when the pressures are above 7 atm. With respect to overpressure, it is claimed that the diaphragm can withstand a pressure unbalance up to 12,500 p.s.i.

To ensure that all the gas in the system was at the same temperature, the indicator was mounted in the oil bath along with the pressure vessels.

Temperature Measurement and Control System. The temperature measurement and control system used in this study was designed and built by Lichtblau (*15*) in the course of his research at Yale University. It consists of a platinum resistance thermometer, a Mueller G-2 bridge, an amplification unit, and a relay circuit.

The operations of temperature measurement and temperature control were incorporated into one system in the following manner. The resistance of the platinum resistance thermometer which corresponded to the desired bath temperature was set on the Mueller bridge. When the bath temperature was not at the set point, there was a potential across the galvanometer terminals of the bridge which was proportional in sign and magnitude to the temperature difference. This potential was then amplified and sent to a relay circuit which activated the heaters.

This control system is a marked improvement over the usual thermoregulator control systems. There is no possibility of the set point's drifting with time, and this system gives a finer control than is possible with a thermoregulator circuit. It was possible to control the temperature to approximately ±0.01° C. at 40°, 50°, and 75° C., and to ±0.015° C. at the higher temperatures.

Gases Used. The helium used for the calibrations was grade A gas with a minimum purity of 99.99%.

The carbon dioxide was the bone-dry grade with minimum purity of 99.8%.

For the 75° and 100° C. runs, research grade ethylene was used. This material is reported to have a typical lot purity of 99.9%. For the other runs, the ethylene used was supplied by the Monsanto Chemical Co. It had a minimum purity of 99.75%. The contaminants were 2000 p.p.m. of ethane and no more than 500 p.p.m. of methane.

RESULTS

Compressibility data were obtained for four mixtures of carbon dioxide and ethylene in a pressure range from approximately 5 to 500 atm. and at 40°, 50°, 75°, 100°, and 125° C. Some runs were also made with the pure components. The experimental compressibility data are presented in Table I.

The data have been fitted by a least squares analysis to high degree polynomials in gas density. These equations fit the data well and can be used for accurate interpolation of the results. The polynomial coefficients and the error variance for each isotherm are presented in Table II, and the details of the curve fitting are given below.

Error Analysis. Errors in the compressibility factor can arise from uncertainties in the following parameters: pressure measurement, temperature measurement, the volumetric constant, *N*, and the zero intercept, *A*.

The maximum error due to the pressure measurement is estimated to be ±0.02% when the low-range gage is used and 0.05% for the high-range gage. For the temperature measurements, the uncertainties are considerably smaller. The maximum temperature deviation of ± 0.015° C. corresponds to an uncertainty of 0.004%.

Table I. Experimental Compressibility Data

40.0° C.

M.F. Ethylene = 0.215		M.F. Ethylene = 0.393		M.F. Ethylene = 0.609		M.F. Ethylene = 0.806		Pure Ethylene	
P, atm.	*Z*	*P*, atm.	*Z*	*P*, atm.	*Z*	*P*, atm.	*Z*	*P*, atm.	*Z*
7.714	0.9664	7.209	0.9689	6.702	0.9703	8.617	0.9603	8.186	0.9621
10.484	0.9537	9.810	0.9574	9.119	0.9585	11.677	0.9449	11.094	0.9467
14.170	0.9359	13.277	0.9408	12.353	0.9428	15.730	0.9242	14.946	0.9260
19.038	0.9129	17.862	0.9190	16.627	0.9214	21.018	0.8966	19.975	0.8986
25.331	0.8820	23.795	0.8889	22.201	0.8933	27.751	0.8596	26.371	0.8614
33.254	0.8407	31.343	0.8502	29.291	0.8557	36.095	0.8118	34.287	0.8131
42.884	0.7872	40.593	0.7994	38.051	0.8071	45.970	0.7506	43.666	0.7519
53.946	0.7190	51.376	0.7346	48.379	0.7451	56.990	0.6757	54.086	0.6762
65.657	0.6353	63.115	0.6553	59.843	0.6692	68.408	0.5889	64.858	0.5888
76.769	0.5394	74.811	0.5640	71.618	0.5815	79.796	0.4988	75.523	0.4978
86.166	0.4396	85.661	0.4689	83.153	0.4902	93.450	0.4241	88.402	0.4231
95.557	0.3539	97.578	0.3878	96.588	0.4134	129.909	0.4281	123.750	0.4300
122.200	0.3286	129.501	0.3737	131.870	0.4098	173.895	0.5049	167.047	0.5115
160.688	0.3808	170.871	0.4345	174.816	0.4788	273.479	0.6999	265.369	0.7162
256.199	0.5351	268.223	0.6011	272.698	0.6582	500.693	1.1297	490.388	1.1667
485.762	0.8945	495.413	0.9788	497.191	1.0580				

50.0° C.

M.F. Ethylene = 0.199		M.F. Ethylene = 0.418		M.F. Ethylene = 0.607		M.F. Ethylene = 0.799	
P, atm.	*Z*	*P*, atm.	*Z*	*P*, atm.	*Z*	*P*, atm.	*Z*
9.389	0.9650	6.315	0.9755	5.944	0.9770	6.415	0.9738
12.739	0.9511	8.608	0.9659	8.110	0.9684	8.741	0.9639
17.199	0.9327	11.695	0.9532	11.027	0.9564	11.864	0.9503
23.053	0.9081	15.812	0.9361	14.918	0.9399	16.016	0.9318
30.574	0.8749	21.220	0.9126	20.047	0.9174	21.459	0.9069
39.987	0.8311	28.230	0.8819	26.694	0.8873	28.460	0.8737
51.309	0.7747	37.063	0.8410	35.117	0.8479	37.233	0.8303
64.182	0.7039	60.330	0.7223	45.429	0.7968	47.828	0.7747
77.791	0.6197	73.986	0.6434	57.523	0.7329	60.018	0.7062
91.017	0.5267	88.125	0.5567	70.921	0.6563	73.326	0.6267
104.251	0.4382	103.286	0.4740	85.126	0.5722	87.586	0.5438
125.578	0.3834	127.923	0.4264	100.938	0.4929	105.527	0.4759
145.529	0.3916	149.204	0.4383	127.296	0.4515	148.168	0.4853
187.664	0.4451	191.214	0.4950	149.790	0.4682	194.100	0.5604
283.471	0.5926	282.346	0.6444	193.451	0.5330	291.636	0.7422
505.011	0.9309	486.320	0.9786	285.969	0.6946	507.508	1.1388
				491.449	1.0525		

(*Continued on page 171*)

Table I. Experimental Compressibility Data (*Continued*)

75.0° C.

Pure Carbon Dioxide		M.F. Ethylene = 0.205		M.F. Ethylene = 0.403		M.F. Ethylene = 0.619		M.F. Ethylene = 0.807	
P, atm.	Z	P, atm.	Z	P, atm.	Z	P, atm.	Z	P, atm.	Z
8.242	0.9762	5.655	0.9834	7.281	0.9791	6.757	0.9794	6.520	0.9799
11.236	0.9667	7.738	0.9774	9.931	0.9701	9.224	0.9713	8.895	0.9711
15.272	0.9544	10.560	0.9689	13.528	0.9600	12.556	0.9603	12.117	0.9609
20.654	0.9376	14.362	0.9572	18.334	0.9450	17.023	0.9458	16.425	0.9461
27.740	0.9147	19.446	0.9414	24.693	0.9245	22.951	0.9262	22.144	0.9265
36.925	0.8844	26.167	0.9202	32.980	0.8969	30.705	0.9001	29.624	0.9004
48.544	0.8446	34.906	0.8916	43.590	0.8611	40.657	0.8657	39.226	0.8660
62.779	0.7934	46.043	0.8543	56.812	0.8152	53.129	0.8218	51.253	0.8219
79.497	0.7298	59.799	0.8060	72.763	0.7584	68.294	0.7673	65.873	0.7673
98.197	0.6548	76.223	0.7462	91.390	0.6919	86.219	0.7036	83.190	0.7039
118.544	0.5742	95.090	0.6762	113.056	0.6218	107.339	0.6363	103.789	0.6379
142.790	0.5024	116.419	0.6014	194.764	0.5652	135.008	0.5813	131.413	0.5867
188.209	0.4810	143.064	0.5368	240.806	0.6159	188.179	0.5886	186.934	0.6062
228.721	0.5152	193.268	0.5268	326.429	0.7359	232.995	0.6423	235.075	0.6719
307.756	0.6111	237.009	0.5694	498.014	0.9899	315.328	0.7663	324.822	0.8184
474.663	0.8309	319.356	0.6762			478.799	1.0258	504.489	1.1207
		486.505	0.9082						

100.0° C.

Pure Carbon Dioxide		M.F. Ethylene = 0.203		M.F. Ethylene = 0.350		M.F. Ethylene = 0.584		M.F. Ethylene = 0.796		Pure Ethylene	
P, atm.	Z	P, atm.	Z	P, atm.	Z	P, atm.	Z	P, atm.	Z	P, atm.	Z
8.289	0.9809	7.738	0.9820	10.139	0.9756	8.354	0.9801	9.003	0.9766	7.137	0.9797
11.328	0.9738	10.581	0.9754	13.828	0.9665	11.400	0.9715	12.286	0.9681	9.757	0.9728
15.441	0.9641	14.427	0.9660	18.801	0.9546	15.529	0.9613	16.712	0.9565	13.295	0.9629
20.964	0.9508	19.612	0.9539	25.444	0.9384	21.069	0.9474	22.629	0.9408	18.047	0.9495
28.320	0.9330	26.525	0.9371	34.221	0.9167	28.438	0.9288	30.459	0.9198	24.379	0.9317
37.991	0.9091	35.651	0.9149	45.653	0.8884	38.103	0.9040	40.679	0.8923	32.709	0.9080
50.496	0.8778	47.504	0.8855	60.273	0.8520	50.604	0.8721	53.788	0.8571	43.502	0.8772
66.310	0.8373	62.611	0.8478	78.575	0.8068	66.447	0.8318	70.288	0.8135	57.227	0.8382
85.784	0.7868	81.391	0.8005	101.035	0.7535	86.162	0.7835	90.745	0.7629	74.334	0.7909
109.142	0.7271	104.291	0.7451	128.724	0.6974	110.620	0.7306	116.438	0.7111	95.502	0.7381
136.959	0.6628	132.119	0.6856	165.636	0.6518	142.423	0.6833	151.960	0.6741	122.644	0.6885
172.667	0.6070	168.656	0.6358	230.007	0.6575	191.668	0.6680	216.624	0.6980	163.596	0.6671
233.537	0.5963	231.246	0.6332	277.678	0.6996	223.687	0.6871	265.905	0.7552	256.200	0.7589
279.055	0.6280	277.434	0.6696	356.845	0.7925	272.251	0.7371	349.021	0.8738	339.458	0.8864
356.388	0.7070	354.460	0.7541	500.335	0.9796	353.249	0.8430	500.904	1.1055	493.408	1.1358
499.919	0.8743	493.738	0.9260			500.429	1.0528				

125.0° C.

Pure Carbon Dioxide		M.F. Ethylene = 0.203		M.F. Ethylene = 0.441		M.F. Ethylene = 0.634		M.F. Ethylene = 0.802	
P, atm.	Z	P, atm.	Z	P, atm.	Z	P, atm.	Z	P, atm.	Z
9.136	0.9822	11.786	0.9772	9.662	0.9814	9.392	0.9799	9.089	0.9809
12.509	0.9764	16.101	0.9693	13.212	0.9744	12.847	0.9732	12.423	0.9734
17.075	0.9678	21.919	0.9581	18.026	0.9653	17.525	0.9640	16.942	0.9639
23.235	0.9561	29.717	0.9431	24.504	0.9528	23.824	0.9514	23.036	0.9516
31.479	0.9405	40.093	0.9238	33.170	0.9364	32.227	0.9345	31.166	0.9347
42.397	0.9198	53.699	0.8984	44.608	0.9144	43.362	0.9129	41.938	0.9133
56.676	0.8927	71.280	0.8659	59.561	0.8864	57.897	0.8850	55.986	0.8852
75.030	0.8581	93.653	0.8260	78.813	0.8517	76.663	0.8509	74.106	0.8508
98.222	0.8156	121.917	0.7808	103.342	0.8108	100.589	0.8106	97.285	0.8109
127.147	0.7666	158.142	0.7354	134.795	0.7679	131.557	0.7698	127.329	0.7706
163.697	0.7166	209.320	0.7067	177.526	0.7343	174.346	0.7407	169.269	0.7438
214.487	0.6817	303.526	0.7440	247.889	0.7445	247.626	0.7639	242.311	0.7731
307.023	0.7086	374.481	0.8090	294.288	0.7789	297.630	0.8091	292.965	0.8237
376.853	0.7665	492.013	0.9369	364.962	0.8513	375.430	0.8994	372.572	0.9232
493.189	0.8841			481.813	0.9905	507.037	1.0707	508.517	1.1107

From Equation 1 it can be seen that the error in Z due to an uncertainty in N of ΔN is proportional to $n\Delta N$, where n is the expansion number. The average deviation of N was ±0.0036%. Therefore, after 13 expansions, the maximum error in Z which can result from this uncertainty is ±0.045%.

Based on the results of the least squares analyses which were used to evaluate the zero intercept, A, the uncertainty in A was never greater than ±0.1% and usually less than ±0.05%. Therefore, when one considers all the possible errors, the Z values are probably accurate to ±0.2%.

Polynomial Representation and Interpolation of Data. For the interpolation of experimental data, it is helpful if the data can be represented by an analytical expression, even a completely empirical one. With an analytical representation of the data it is a simple matter to check the precision of the results and interpolate the data accurately.

The first attempt at fitting the data to an equation involved the use of Equation 4. Although the polynomial degree was increased up to eight, it was still not possible to obtain a good fit. The next attempt involved the use of an equation of state which represents the compressibility factor as a polynomial in gas density D:

$$Z = 1 + B''D + C''D^2 \dots \tag{9}$$

which was found to fit the data accurately if polynomials of high degree were used.

Table II. Polynomial Coefficients Resulting from Least Squares Analysis of Compressibility Data

$$Z = 1 + a_1 D + a_2 D^2 + a_3 D^3 \ldots$$

D = gas density, lb. moles/cu. feet

A. 40° C.

Term	21.5% C_2H_4	39.3% C_2H_4	60.9% C_2H_4	80.6% C_2H_4	100% C_2H_4
a_1	−1.779172	−1.778275	−1.850607	−1.895080	−1.922767
a_2	1.264004	1.153303	1.384111	1.283397	0.561196
a_3	0.266621	0.966938	0.967320	1.814156	5.898995
a_4	−0.358558	−1.328235	−1.979881	−3.419548	−12.488754
a_5	−0.768135	−0.853102	−0.007009	0.739099	10.567515
a_6	0.723895	1.942545	1.767264	2.222051	−2.549225
a_7	0.170957	−0.624912	−0.636421	−0.904979	
a_8	−0.154789				
Error variance	1.06×10^{-5}	2.80×10^{-5}	2.17×10^{-5}	2.86×10^{-5}	6.85×10^{-6}

B. 50° C.

	19.9% C_2H_4	41.8% C_2H_4	60.7% C_2H_4	79.9% C_2H_4
a_1	−1.589052	−1.658586	−1.655661	−1.734538
a_2	0.727749	1.177917	0.819159	1.011881
a_3	1.756106	0.566113	2.541549	2.521372
a_4	−3.169594	−0.842530	−5.101036	−5.505389
a_5	2.060103	−0.827674	3.846835	4.410886
a_6	−0.334647	1.713240	−0.691236	−0.752577
a_7		−0.533499		
Error variance	1.70×10^{-5}	5.82×10^{-6}	1.97×10^{-5}	7.24×10^{-6}

C. 75° C.

	100% CO_2	20.5% C_2H_4	40.3% C_2H_4	61.9% C_2H_4	80.7% C_2H_4
a_1	−1.335891	−1.334506	−1.327987	−1.419324	−1.460085
a_2	0.709710	0.719106	0.436703	1.006084	0.944631
a_3	0.881790	1.181409	2.820804	1.156903	1.850534
a_4	−1.593999	−2.267591	−5.377313	−2.687173	−3.981790
a_5	0.985620	1.616788	4.233179	2.231322	3.339232
a_6	−0.116216	−0.274355	−1.002123	−0.315866	−0.514194
Error variance	6.92×10^{-6}	3.07×10^{-6}	2.37×10^{-5}	6.43×10^{-6}	1.27×10^{-5}

D. 100° C.

	100% CO_2	20.3% C_2H_4	35.0% C_2H_4	58.4% C_2H_4	79.6% C_2H_4	100% C_2H_4
a_1	−1.124070	−1.131997	−1.169252	−1.202544	−1.257146	−1.352694
a_2	0.631564	0.708195	0.981246	0.940748	0.950671	1.323495
a_3	0.769315	0.847348	0.126064	0.919560	1.505069	0.457462
a_4	−1.467872	−1.808974	−0.638173	−2.227279	−3.570991	−1.596358
a_5	1.059987	1.500769	0.605318	2.051237	3.472902	1.761710
a_6	−0.184719	−0.315685		−0.351436	−0.751060	
Error variance	6.41×10^{-7}	1.19×10^{-6}	1.13×10^{-6}	7.76×10^{-6}	1.14×10^{-6}	3.82×10^{-6}

E. 125° C.

	100% CO_2	20.3% C_2H_4	44.1% C_2H_4	63.4% C_2H_4	80.2% C_2H_4
a_1	−0.980932	−0.995511	−1.008356	−1.084032	−1.111935
a_2	0.792061	0.927731	0.992908	1.485963	1.481057
a_3	−0.003757	−0.153985	−0.244178	−1.831611	−1.580096
a_4	−0.283059	−0.184807	0.348592	3.428488	3.231091
a_5	0.290487	0.338760	V0.331586	−3.148965	−3.192415
a_6			0.365966	1.464158	1.675753
Error variance	5.06×10^{-6}	5.15×10^{-6}	2.27×10^{-6}	1.25×10^{-5}	6.97×10^{-6}

Each isotherm, which contained from 13 to 17 data points, was fitted to polynomials in gas density of fourth through eighth degree by a least squares analysis. The computations were done on an IBM 709 digital computer. The criterion used to pick the degree of polynomial which best represented the data was the value of the error variance, σ^2. In these calculations, error variance is defined as (*14*)

$$\sigma^2 = \frac{S_m^2}{M - (m + 1)} \qquad (10)$$

where

S_m = sum of the square of the residuals

M = number of data points

m = degree of the polynomial

It was found that the error variance passed through a minimum as the polynomial degree was increased. The polynomial degree that produced the minimum variance was considered as the best fit of the data.

As the temperature of the system decreased and approached the critical temperature of the gas or gas mixture, it became more difficult to represent the data analytically. This was reflected in the increased magnitude of the error variance. In general, as mixtures became richer in carbon dioxide, it was also more difficult to fit the data. However, even for the poorest fit, the deviations did not exceed 0.1%, and for most of the experimental points they were less than 0.03%. Since this is well within the experimental uncertainty associated with the compressibility factor, these polynomials can be safely used for interpolation of the compressibility data.

Comparison of Data with Results of Other Investigators. The compressibility of ethylene was measured at 100° C.

and compared with Michels' results. For the 15 experimental points, the average deviation was 0.1%, with a maximum error of 0.2%. Our carbon dioxide data at 100° C. were also compared with Michels' data and the deviations were essentially the same as with the ethylene. Part of this error is attributed to the fact that the gases used in this study were not of ultimate purity.

Seven calibrations were conducted with helium at 100° C. The second virial coefficients were computed and the average value is compared to the values determined by Ku and Dodge (*13*), Michels and Wouters (*21*), Schneider and Duffie (*28*), and Wiebe and coworkers (*31*) in Table III. The differences between the value obtained in this work and those by other investigators shown in Table III are within the experimental uncertainty of this work.

Ku (*12*) measured the compressibility of three carbon dioxide–ethylene mixtures at 100° C. at pressures up to 260 atm. To compare these data with those of the present study, Ku's compressibility factors were fitted to a polynomial in density and interpolated to even intervals of pressure. It was then possible to compare the Z *vs.* composition behavior of the two investigations (Figure 2). Ku's values of Z for 30% ethylene deviate as much as 2.5% from the present results. Possible causes of these large deviations are leakage during the run or incomplete mixing. For his runs in mixtures containing 75 and 88% ethylene, the maximum deviation from our results is approximately 0.6%, but most of the points are within 0.2% of the values determined in this study.

Evaluation of Second Virial Coefficients. True second virial coefficients are obtained from a limiting process in which PVT data are extrapolated to $p = 0$. Depending on the range of pressures and the method of extrapolation, considerable variation in the coefficients between different experimenters is to be expected. Many authors have not been careful to point out how their values were obtained. We make no special claim for the accuracy of our values, but at least we used only the lower range of pressures of our experiments and made the extrapolation by the best procedure that we could devise.

Table III. Second Virial Coefficient of Helium at 100° C.

Investigator	$B \times 10^4$, Atm.$^{-1}$
This work	3.69 ± 0.05
Ku and Dodge (*13*)	3.88
Michels and Wouters (*21*)	3.71
Schneider and Duffie (*28*)	3.73
Wiebe and coworkers (*31*)	3.69

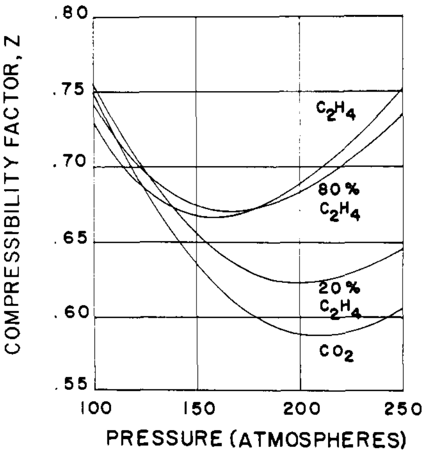

Figure 2. Compressibility of CO_2–C_2H_4 mixtures at 100° C.

In the process of evaluating the zero intercept, A, by fitting the low pressure compressibility data to Equation 8, values of the second virial coefficient have been obtained. The experimental values for the pure gases are compared to those of other investigators in Table IV. Except for ethylene at 40° C., the difference between these values is well within the experimental uncertainty of this work.

The second virial coefficients for the mixtures were also evaluated and are presented in Table V. Excluding the values for the 40° and 50° runs because of the scatter in the data, the remainder of the values were used to evaluate the interaction coefficient B_{12} using our own B_1 and B_2 values, except for C_2H_4 at 75° and 125° C., where the values of Michels and Geldermanns (*19*) were used. A least-squares technique was used for the evaluation. The B_{12} values so derived are compared in Table VI with three empirical mixing rules and one semi-empirical rule based on averaging the force constants in the Lennard-Jones potentials for the two pure gases (*10*).

The comparison reveals that all four rules predict essentially the same values and therefore no one can be considered superior to the others in predicting the value of B_{12}. The values given for the Lennard-Jones approach are based on force constants which best fit the data at the three

Table IV. Comparison of Our Pure Component B Values with Those of Others

Gas	Temp., ° C.	$B \times 10^3$, Atm.$^{-1}$ This work	$B \times 10^3$, Atm.$^{-1}$ Other
CO_2	75	-2.86	-2.98[a] (*17*)
			-3.04 (*20*)
	100	-2.28	-2.32[a] (*17*)
			-2.40 (*20*)
			-2.53 (*13*)
	125	-1.88	-1.81[a] (*17*)
			-1.90 (*20*)
C_2H_4	40	-4.52	-4.92[b] (*19*)
	100	-2.77	-2.77 (*19*)
			-2.85 (*13*)

[a] Calculated from equation in (*17*). [b] Interpolated value.

Table V. Second Virial Coefficients of Mixtures

($B \times 10^3$, atm.$^{-1}$)

Mole Fraction Ethylene	Temperature, ° C. 40	50	75	100	125
0.0	...	...	-2.86	-2.28	-1.88
0.2	-4.24	-3.60	-2.87	-2.31	-1.93
0.4	-4.13	-3.83	-2.86	-2.40	-1.94
0.6	-4.36	-3.75	-3.07	-2.47	-2.07
0.8	-4.40	-3.97	-3.15	-2.57	-2.14
1.0	-4.52	...	-3.49[a]	-2.77	-2.21[a]

[a] Evaluated from data of Michels and Geldermanns (*19*).

Table VI. Interaction Coefficient Data

	$B_{12} \times 10^3$, Atm.$^{-1}$ 75° C.	100° C.	125° C.
Experimental	-2.70	-2.33	-1.96
Predicted by			
$B_{12} = (B_1 + B_2)/2$	-3.18	-2.53	-2.05
$B_{12} = (B_1 B_2)^{1/2}$	-3.16	-2.51	-2.04
$B_{12} = = \frac{1}{8}(B_1^{1/3} + B_2^{1/3})^3$	-3.16	-2.52	-2.04
Averaging of Lennard-Jones Potential constants	-3.22	-2.58	-2.10

temperatures shown. The fact that all four methods give similar results is not surprising, since the values of B for the pure components are not greatly different. It is probably more surprising that the values of B_{12} predicted by these methods do not agree very well with those obtained from experimental data. The difference between predicted and experimental values of B_{12} increases as the temperature decreases. A comparison of Tables V and VI also shows that the values of B_{12} lie much closer to the values for carbon dioxide than those for ethylene, and at 75° C. the value of B_{12} actually lies outside the range of pure component values. These trends are explained below.

The Lennard-Jones model assumes spherical symmetry and considers central forces only. A more realistic model should account for the physical shape of the molecules involved. As a step in this direction calculations were first made for Corner's four-center model for long molecules using the constants given by Hirschfelder, Curtiss, and Bird (*10*). The significant point revealed by these calculations was that values of B_{12} were again approximately the arithmetic mean of the pure component values. In order to have a value of B_{12} much nearer the value of one of the pure components than the other, where the pure component values are of comparable magnitude, some significant contributions to the second virial coefficient of that pure component must be zero or very small for the interaction between unlike molecules. Such an effect could be due to the quadrupole-quadrupole interaction of CO_2 molecules, which is known to be significant. If it is assumed further that ethylene has a negligible quadrupole moment, giving a negligible unlike interaction term, then the experimental trends described above can be explained. Although there is general agreement in the literature that the quadrupole-quadrupole effect for CO_2 is significant, there is disagreement as to the actual quantitative contribution. Depending upon the potential model used, the quadrupole moments selected from the literature, and the inclusion or omission of non-central forces in addition to the quadrupole-quadrupole one, values of the contribution to the second virial coefficient of the quadrupole-quadrupole effect vary from about 7 to 50% of the total value for CO_2 at 100° C. In all cases the total second virial coefficients agree well with each other. Results based on the approach used by Prausnitz and Myers (*25*) (Table VII) show that the quadrupole-quadrupole effect can explain the trends in the experimental values of B_{12} described above. This approach uses the Kihara potential combined with a quadrupole-quadrupole correction based on the work of Pople (*24*). Prausnitz and Myers used a spherocylinder core for CO_2 and a rectangular one for ethylene. The quadrupole moment of ethylene was taken as zero.

No attempt was made to fit the data of the present work to the model described above. The values in Table VII were obtained from constants given by Pople (*24*). Consequently, the trends in the results given in Table VII and not the absolute values should be compared with the results in Tables V and VI. For both temperatures the values of B_{12} lie close to those for CO_2 and the difference between B_{12} and B_{CO_2} becomes smaller the lower the temperature. The calculated difference is the same as the experimental one at 100° C. Our results at 75° C. indicate a greater contribution of the quadrupole-quadrupole effect than that predicted by the above model.

Table VII. Second Virial Coefficients Calculated by Method of Prausnitz and Myers

	$B_{C_2H_4}$ 10^3 Atm.$^{-1}$	B_{12} 10^3 Atm.$^{-1}$	B_{CO_2} 10^3 Atm.$^{-1}$
100° C.	-2.69	-2.49	-2.44
75° C.	-3.45	-3.19	-3.17

Discussion of Mixture Results. The compressibility factors of both carbon dioxide and ethylene pass through a minimum in the pressure and temperature ranges studied. For this reason, the plots of Z *vs.* pressure for the pure gases and the mixtures intersect at many points. Since these plots are cluttered, only one set is presented in order to illustrate the general trends in the data. The compressibility *vs.* pressure results for the carbon dioxide–ethylene system at 100° C. over a limited pressure and composition range are shown in Figure 3.

It can be seen from this figure that for a wide range of pressure, the compressibilities of the mixtures are greater than the compressibilities of either of the two pure components, at all the temperatures studied. This behavior is not unique to this system, but occurs with many gas mixtures, such as the nitrogen-helium (*11, 12*) and the propane-nitrogen systems (*30*). At present all of the common rules for predicting mixture compressibility results yield values in between those of the pure components. These rules obviously cannot accurately represent this type of system.

Test of Mixing Rules. ADDITIVE-VOLUME LAW. Dodge (*6*) has shown that the following method of combining compressibility factors to predict mixture behavior follows directly from the additive-volume law:

$$Z_m = X_A Z_A + X_B Z_B \tag{11}$$

where Z_A and Z_B are the pure component compressibility factors evaluated at the temperature and pressure of the mixture. This method of combining compressibility factors is commonly used, since no trial and error calculations are required if the pure component compressibility factors are known or can be estimated. It was tested on one mixture at 40° C. and another at 125° C. As indicated previously, this method is poor in the region where the crossovers in compressibility occur. At 40° C. the maximum deviation of 12.9% occurs at 100 atm., and at 125° C. the maximum deviation of 2.1% occurs at 200 atm.

BENEDICT-WEBB-RUBIN EQUATION OF STATE. The eight-constant BWR equation of state (*1*) is of considerable interest, since it can accurately represent the PVT properties of pure hydrocarbons in the gas and liquid phases over wide ranges of pressure and temperature. The authors (*2*) have suggested that their equation of state can be used for mixtures if the constants of the equation for the pure components are combined in the proper manner. They proposed the following empirical rules for combining constants:

B_0	Linear combination	
A_0, C_0, γ	Linear square root	$k_m = [\Sigma(x_i k_i^{1/2})]^2$
a, b, c, α	Linear cube root	$k_m = [\Sigma(x_i k_i^{1/3})]^3$

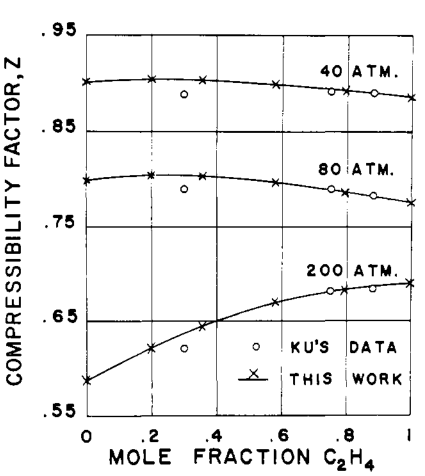

Figure 3. Compressibility vs. pressure for CO_2–C_2H_4 system at 100° C.

Table VIII. B-W-R Constants for Mixtures Evaluated from Experimental Data

	Mole Fraction Ethylene					
Constant	0	0.2	0.4	0.6	0.8	1.0
$B_0 \times 10$	3.3059338	0.73907351	0.18860239	2.4058934	0.46198813	3.8863540
$A_0 \times 10^{-3}$	0.39383876	0.24390572	0.21064826	0.39902797	0.27755299	0.54363699
$C_0 \times 10^{-8}$	0.44705108	0.47554571	0.49942181	0.42171649	0.49560086	0.41789345
$b \times 10^{-1}$	0.15482312	0.16849756	0.19535999	0.20358153	0.22580405	0.25721440
$a \times 10^{-4}$	0.08595546	0.08584442	0.09902589	0.09533699	0.10496643	0.12069940
$a\alpha \times 10^{-3}$	0.15374392	0.19042768	0.27232805	0.36171757	0.49321856	0.66171740
$c \times 10^{-8}$	0.65039053	0.58745542	0.65068244	0.62632373	0.68679676	0.78453399
γ	1.0012031	1.1288749	1.2982524	1.5663242	1.7723799	1.9652156

Units used in B-W-R equation: P = atmospheres, v = cu. ft. per lb. mole, T = ° K.

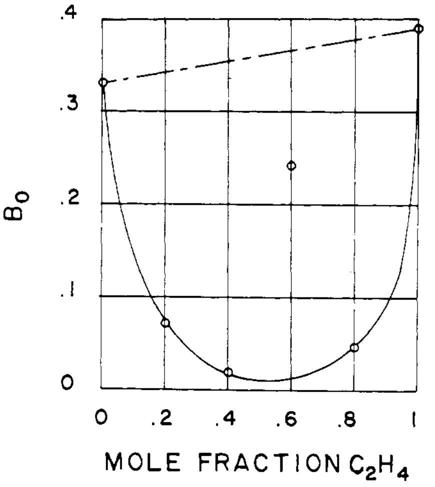

Figure 4. B_0 *vs.* composition for CO_2–C_2H_4 mixtures

(Temperature = 50° to 125° C.)

Table IX. Deviation between Experimental and B-W-R Predicted Z Values

Mole Fraction Ethylene	Av. % Deviation	Max. % Deviation
0	0.38	1.08
0.2	0.29	0.91
0.4	0.27	0.80
0.6	0.37	1.21
0.8	0.26	0.74
1	0.22	0.65

These rules have had moderate success when used with hydrocarbon mixtures.

Although the equation was developed for use with hydrocarbons, it has been tested on other pure components with some success. However, the prediction of mixture properties based on the above mixing rules has given very poor results for systems which are not entirely composed of hydrocarbons. Eakin and Ellington (7) studied the application of the BWR equation to carbon dioxide–hydrocarbon mixtures using the proposed mixing rules. Four gas-phase systems were studied at pressures up to 3000 p.s.i.a. at temperatures from 60° to 460° F. To obtain a reasonable fit of the mixture data, they had to develop two sets of BWR constants for the carbon dioxide, one for mixtures containing less than 40% carbon dioxide and another for the remaining mixtures. Even with these two sets of constants, the rich carbon dioxide mixtures had an average pressure deviation of 2.76%.

These investigators probably had difficulty in fitting the mixture data because they forced the data to obey the proposed mixing rules. Therefore another approach has been used in this study. The BWR constants were calculated for each of the four mixtures as well as the pure components in the temperature range of 50° to 125° C. In these computations, pressure was expressed in atmospheres, specific volume in cubic feet per pound mole, and temperature in ° K. Since the experimental data were not taken at exactly the same composition at each temperature, it was first necessary to interpolate the Z *vs.* composition data to even increments of composition. The BWR constants were then computed by a least-squares analysis developed by Sage and coworkers (*3, 23, 29*). Digital computer programs have been developed at Yale for these calculations by Long (*16*) and Ryan (*27*). The use of these programs indicated that double precision arithmetic was required for these calculations. Round-off error in the single precision program yielded constants which deviated by more than 100% from the values computed by the double precision program.

The computed constants presented in Table VIII should be useful to anyone working with this mixture, and they also show that the trend in the constants with composition is different from that expected from the mixing rules. This is illustrated for one case in Figure 4, where the variation of the constant B_0 with composition is shown. In plotting the curve we have ignored the point for $X = 0.60$ which, for some reason we are unable to explain, deviates from the general trend. It is evident that the BWR mixing rules are inadequate for this system, since they cannot predict the apparent maxima and minima which occur for the constants A_0, B_0, C_0, and c. This behavior is certainly due in part to the quadrupole-quadrupole effect described above. However, since the BWR equation of state includes the effect of virial coefficients higher than the second, the phenomenon is necessarily more complex than that described.

Using the constants in Table VIII, we have compared the calculated values of Z with our experimental values (Table IX). It is evident that the BWR equation can represent mixture data about as well as pure component data, provided the constants are evaluated directly from mixture data and not calculated by mixing rules.

ACKNOWLEDGMENT

The junior author gratefully acknowledges financial aid from the National Science Foundation Grant for High Pressure Research 1960–1961 and the United States Steel Fellowship 1961–1963.

NOMENCLATURE

A = zero intercept
A_0 = constant in BWR equation of state
a = constant in BWR equation
B = second virial coefficient defined by Equation 4
B' = second virial coefficient defined by Equation 3
B'' = second virial coefficient defined by Equation 7
B_0 = constant in BWR equation of state
b = constant in BWR equation of state
C = third virial coefficient defined by Equation 4
C' = third virial coefficient defined by Equation 3
C'' = third virial coefficient defined by Equation 7
C_0 = constant in BWR equation of state
c = constant in BWR equation of state
D = gas density, lb. moles per cubic foot
D' = fourth virial coefficient in Equation 3
M.F. = mole fraction
N = volumetric constant
P = pressure, atmospheres
X_A = mole fraction of component A in a mixture
Z = compressibility factor
γ = constant in BWR equation of state
α = constant in BWR equation of state

Subscripts and Exponents

n = number of expansions
$^\circ$ = initial conditions

LITERATURE CITED

(1) Benedict, M., Webb, G.B., Rubin, L.C., *J. Chem. Phys.* **8**, 334-45 (1940).
(2) *Ibid.*. 10, 747-758 (1942).
(3) Brough, H.W., Schlinger, W.G., Sage, B.H., *Ind. Eng. Chem.* **43**, 2442-66 (1951).
(4) Burnett, E.S., *J. Appl. Mech.* **58**, A136-42 (1936).
(5) Dick, W.F.L., Hedley, A.G.M., "Thermodynamic Functions of Gases," Vol. **II**, pp. 88-114, Butterworth, London, 1956.
(6) Dodge, B.F., "Chemical Engineering Thermodynamics," p. 194, McGraw-Hill, New York, 1944.
(7) Eakin, B.E., Ellington, R.T., "Thermodynamic and Transport Properties of Gases, Liquids, and Solids," pp. 195-204, McGraw-Hill, New York, 1959.
(8) Harper, R.C., Miller, J.G., *J. Chem. Phys.* **27**, 36-9 (1957).
(9) Heichelheim, H.R., McKetta, J.J., Jr., *Chem. Eng. Progr. Symp. Ser.* **59** (44), 23-9 (1963).
(10) Hirschfelder, J.O., Curtiss, C.F., Bird, R.B., "Molecular Theory of Gases and Liquids," pp. 131-234, Wiley, New York, 1954.
(11) Kramer, G.M., Miller, J.G., *J. Phys. Chem.* **61**, 785-8 (1957).
(12) Ku, P.S., "Pressure-Volume-Temperature Relationships of Gas Mixtures," D. Eng. dissertation, Yale University, 1960.
(13) Ku, P.S., Dodge, B.F., personal communication.
(14) Lapidus, L., "Digital Computation for Chemical Engineers," pp. 328-30, McGraw-Hill, New York, 1962.
(15) Lichtblau, L.M., "Compressibility of Ammonia and its Mixtures with Nitrogen," D. Eng. dissertation, Yale University, 1963.
(16) Long, L.J., Yale University, New Haven, Conn., private communication, 1963.
(17) MacCormack, K.E., Schneider, W.G., *J. Chem. Phys.* **18**, 1269 (1950).
(18) Michels, A., DeGruyter, J., Niesen, F., *Physica* **3**, 346-51 (1936).
(19) Michels, A., Geldermanns, M., *Ibid.*, **9**, 967-73 (1942).
(20) Michels, A., Michels, C., *Proc. Roy. Soc. (London)* **153A**, 201-14 (1935).
(21) Michels, A., Wouters, H., *Physica* **8**, 923-32 (1941).
(22) Newitt, D.M., Pai, M.O., "Thermodynamic Functions of Gases," Vol. **I**, pp. 102-34, Butterworth, London, 1956.
(23) Opfell, J.B., Sage, B.H., *Ind. Eng. Chem.* **50**, 803-6 (1958).
(24) Pople, J.A., *Proc. Roy. Soc. (London)* **A221**; 508 (1954).
(25) Prausnitz, J.M., Myers, A.L., *A.I.Ch.E. J.* **9**, 5-11 (1963).
(26) Reamer, H.H., Sage, B.H., Lacey, W.N., *Ind. Eng. Chem.* **36**, 88-90 (1940).
(27) Ryan, D., Yale University, New Haven, Conn., private communication, 1963.
(28) Schneider, W.G., Duffie, J.A.H., *J. Chem. Phys.* **17**, 751-54 (1949).
(29) Sellick, F.T., Opfell, J.B., Sage, B.H., *Ind. Eng. Chem.* **45**, 1350-4 (1953).
(30) Watson, G.M., Stevens, A.B., Evans, R.B., Hodges, D., Jr., *Ibid.*, **46**, 362-4 (1954).
(31) Wiebe, R., Gaddy, V.L., Heins, C., *J. Am. Chem. Soc.* **53**, 1721 (1931).

RECEIVED for review December 15, 1965. Accepted December 14. 1966. Continuation of work initiated at Yale University by P.S. Ku under the direction of B.F. Dodge (*12*).

Excess Volume of Mixing of *n*-Alkane Mixtures

CHARLES HARRISON[1] and JACK WINNICK
Department of Chemical Engineering, University of Missouri, Columbia, Mo.

The excess volume of mixing for five normal alkane mixtures was determined by pycnometric technique. The mixtures investigated were the normal alkane mixtures C_{10}-C_{12}, C_{12}-C_{14}, C_{10}-C_{14}, C_{12}-C_{16}, and C_{10}-C_{16}. The investigations were carried out at three temperatures, 25°, 35°, and 45° C., over the entire range of compositions. A volume contraction was observed in all cases, ranging up to −0.14 cc. per mole. The maximum error observed was 0.008 cc. per mole or about 0.0032% of the total volume. The data were correlated using equations based on the principle of congruence. Deviations averaged about 0.002 cc. per mole.

THE MOST successful correlative technique for the thermodynamic excess properties of liquid mixtures was postulated by Brønsted and Koefoed (*1*) in 1946 for alkane mixtures; however, this technique could apply to chain molecules in general. Only Brønsted and Koefoed's own vapor pressure data and heat of mixing data by Van der Waals and Hermans (*8*) were available until the late 1950's when Desmyter and Van der Waals (*3*) measured the volume changes on mixing for six alkane mixtures. These data bore out Brønsted's principle of congruence, at least for short-chain-length molecules at moderate temperatures.

THEORY

Brønsted postulated that the excess thermodynamic properties were a function of the index of the mixture. This index is equal to the average chain length and is defined by the equation:

$$N = \sum_i N_i x_i \qquad (1)$$

N_i is the number of carbon atoms in the chain of the ith species and x_i is the mole fraction of that species. Brønsted called this theory the principle of congruence, according to

---

[1] Present address: Texaco, Inc., Port Arthur, Tex.